GeoPlanning
Journal of Geomatics and Planning
Vol. 9, No. 1, 2022

e-ISSN: 2355-6544

Received: 24 September 2021;
Accepted: 22 November 2022;
Published: 29 November 2022.

Keywords:
Terrestrial Laser Scanner, Unmanned Aerial Vehicle, Data Integration, Point Cloud, 3D Model

*Corresponding author(s)
email: ayujessy@itenas.ac.id

Original Research Open access

3D Modelling of Boscha Observatory with TLS and UAV Integration Data

Gusti A. J. Kartini[1]*, Naura D. Saputri[1]

1. *Department of Geodetic Engineering, Faculty of Civil Engineering and Planning, Institut Teknologi Nasional Bandung, Indonesia*

DOI: 10.14710/geoplanning.9.1.37-46

Abstract

The Bosscha Observatory is Southeast Asia's first modern astronomical observatory. This observatory is located exactly on the Lembang Fault in West Java, Indonesia. Its existence on the fault line makes Bosscha Observatory very vulnerable to disasters, which in the future will cause severe damage to the cultural heritage building. One way to protect the preservation of cultural heritage buildings is through 3D digital documentation. With 3D shapes, we can obtain precise visual and geometric data that can be used to monitor the building's condition. There are two technologies will be used in this study, terrestrial laser scanner (TLS) and unmanned aerial vehicle (UAV) photogrammetry. TLS systems can capture millions of points representing 3-D coordinates at extremely high spatial densities on complex, multidimensional surfaces within minutes. UAV photogrammetry can generate 3D point cloud in centimeter-level precision. The results of data integration between TLS and UAV have been implemented successfully and can be used as one of the measurement techniques supporting 3D modeling and compensating for the shortcomings of each tool. This three-dimensional model can be used to create a cylindrical portion of a building and the roof of a hemispherical building; the texture and color of the building's details, such as windows, doors, and stairs, can be produced with an RMSE error value of 0.025 meters.

Copyright © 2022 GJGP-Undip
This open access article is distributed under a
Creative Commons Attribution (CC-BY-NC-SA) 4.0 International license

1. Introduction

The Bosscha Observatory is Southeast Asia's first modern astronomical observatory, having been designated as a National Cultural Heritage site in 2004 and a National Vital Object in 2008. This observatory is located exactly on the Lembang Fault in West Java, Indonesia (Figure 1). According to research, this fault can produce earthquakes with a magnitude of 6.5–7.0 on the Richter scale (Daryono et al., 2019). Its existence on the fault line makes Bosscha Observatory very vulnerable to disasters, which in the future will cause severe damage to the cultural heritage building. Because of the importance of cultural heritage buildings for the future, protection is needed to prevent damage and destruction (Batur et al., 2020; Chmutina et al., 2020). One way to protect the preservation of cultural heritage buildings is through digital documentation.

Typically, image-based technology or lasers have been utilized in the documentation of cultural heritage structures. With the aid of this technology, the documentation results are not only 2D but also 3D. The researcher was able to accurately document their subjects using 3D digital data formats (Dostal & Yamafune, 2018). With 3D shapes, we can obtain precise visual and geometric data that can be used to monitor the building's condition (Kushwaha et al., 2020). The high precision of measurement makes it possible to investigate the deformations and damages of historic objects (Kwoczynska et al., 2016).

Wirnajaya et al. (2019) conducted 3D mapping at the Bosscha Observatory using Terrestrial Laser Scanner (TLS) technology to produce the majority of 3D point cloud shapes. The absence of point cloud data on the roof of the Bosscha Observatory is a limitation of their research. In other studies, to obtain the top or difficult-

to-scan areas of an object, additional tools such as cranes are required (Büyüksalih et al., 2020). TLS scanning is relatively more expensive in terms of cost, but it has many advantages, including the ability to map quickly and in large quantities, to provide position, intensity, and RGB information, and to produce relatively precise measurements (Wu et al., 2021). TLS systems can capture millions of points representing 3-D coordinates at extremely high spatial densities on complex, multidimensional surfaces within minutes (Gallay et al., 2015). The technology can quickly determine the precise coordinates of points that represent the surface of an object (Klapa et al., 2017).

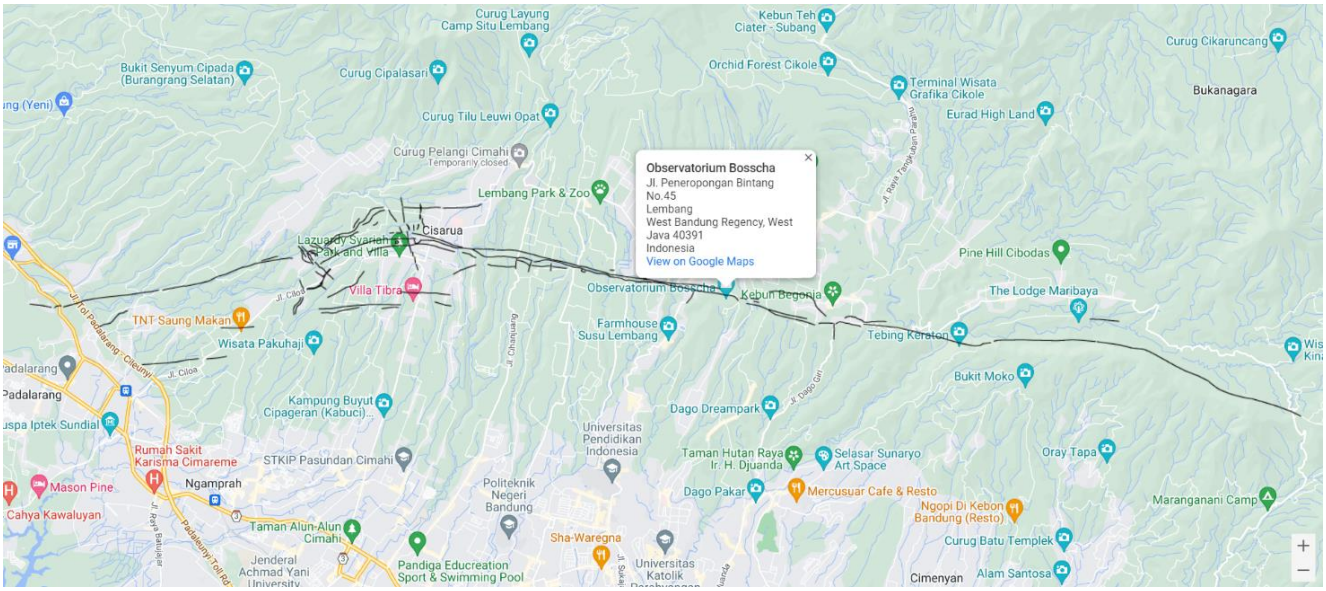

Source: Daryono et al., 2018

Figure 1. The location of the Bosscha Observatory (6°49'28.97" S 107°37'01.59" E) is on the Lembang Fault trajectory. The Lembang Fault is illustrated with a black line that stretches for 29 km

In addition to TLS, Maharani et al. (2020) have used Unmanned Aerial Vehicle (UAV) photogrammetry to document the Bosscha Observatory and produce its full 3D shape. The resulting photographs were then combined and converted into a point cloud shape using Agisoft Metashape in this study. In other studies, photography-based technologies are commonly used to document heritage building (Febro, 2020; Manajitprasert et al., 2019; Themistocleous, 2020). This is because UAV photogrammetry is relatively inexpensive, in addition to being simple to operate and capable of producing high-quality 3D models (Manajitprasert et al., 2019; A Murtiyoso et al., 2019). 3D point clouds can be reconstructed from UAV images with satisfactory accuracy; these images can generate centimeter-level precision (Arnadi Murtiyoso & Grussenmeyer, 2017; Pan et al., 2019).

In a separate study, a combination of TLS and UAV was utilized to create 3D documentation of historical buildings. Ulvi (2021) combines UAV and TLS data because TLS is incapable of obtaining roof and tower area. According to the findings of Ulvi (2021) it is known that the two techniques can complement each other. Hu et al. (2016) merged point cloud data from multiple technologies on the Liyang Yi Temple building, Wudang Mountain, Shiyan, Hubei Province, Central China, to determine the building's complete shape. Complex architectural structures may be restored using a combination of different technologies (AĞCA et al., 2020; Li et al., 2021; Liang et al., 2018).

The integration of TLS and UAV is possible based on previous research. The Bosscha Observatory has point cloud data and photographs, but there is no research on creating 3D models of the building, so this study will attempt to combine the two data sets. The results of this study will be compared with data from Wirnajaya et al. (2019) to determine if the results of this integration are better to those of previous studies.

2. Data and Methods

We utilized secondary data from previous studies for this investigation. In March of 2019, scans were performed using a Topcon GLS-2000 TLS. This results of the study conducted ten scans in the.e57 data format (Figure 2a). In April 2019, scanning with a DJI Mavic 2 Pro UAV and ground control point (GCP) coordinate measurements were performed. The scan produced 334 images in .JPEG format and 31 coordinate points in the WGS 84/UTM Zone 48S system (Figure 2b).

Afterward, data processing is performed on each data set. The cloud-to-cloud method is used to perform a registration process for TLS data processing in Cyclone 2020, after which the accuracy of the values generated by the registration process is evaluated. Then, a filtering process is applied to eliminate noise from building objects that are no longer required or will be removed in order to concentrate on the desired area.

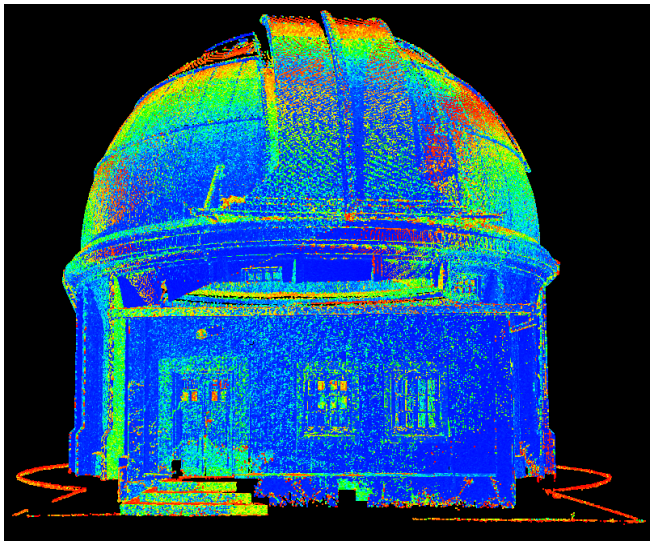

(a)

(b)

Source: Analysis, 2022

Figure 2. (a) TLS scan result and (b) UAV photogrammetry scan result.

Furthermore, photogrammetric data processing is carried out on Agisoft Metashape. The first step in UAV data processing is the align photos procedure, which is used to identify the image's points. This method matches points from two or more photographs. This process will generate a useful initial three-dimensional model in the form of a sparse point cloud for the subsequent stage. Following the process of aligning photos, the georeferencing stage is performed to provide a three-dimensional X, Y, and Z coordinate reference for the aligned photos. This phase also includes the marking of photographs, which is used to identify GCP points on the photograph. The location of the marker is determined by the point measured in the field using an object that is readily identifiable. Then, the process of optimizing cameras is executed, which aims to realign the photos from the preceding process (marking photos and geofencing), which are adjusted to the precision of the camera's position from the selected coordinate system. In addition, the process of forming dense point clouds produces point clouds with a greater density than sparse point clouds.

The integration of TLS and UAV data is the subsequent step, which is performed on CloudCompare. Generally, processing is performed using the method depicted in Figure 3. The entered data are already in the same coordinate system, WGS 84/UTM Zone 48S, because the research area is in Lembang, West Java. The data format generated by the TLS data processing is a point cloud in e57 format, while the data format generated by the UAV data processing is a dense point cloud in e57 format. The e57 format was selected because it is a compact and vendor-neutral file format used for storing and exchanging three-dimensional (3D) imaging data, including point clouds, images, and metadata. Numerous applications support the e57 data format.

The next step is data integration using merge points, so that the data generated by TLS and UAV are merged into a single set. To combine the two measurements' data, it is essential that the resulting point cloud data have the same coordinate system. Using the Point Pairs Picking registration method, the data integration procedure is carried out by selecting the elements of the most prominent object between the two datasets. On the edges (edges of the building) and corners of the building, it is possible to select object elements. There are a total of 10 points used in the registration process. This registration procedure results in an accuracy of 0.025 meter. The total number of points resulting from this integration is 213,286,187.

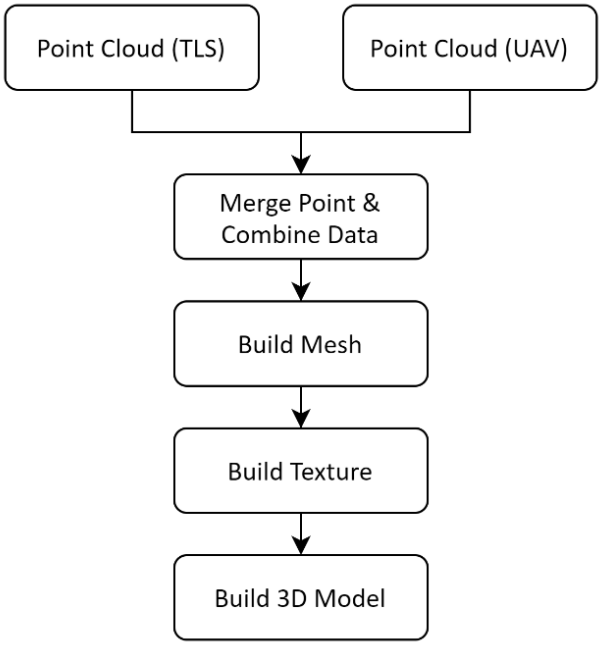

Source: Analysis, 2022

Figure 3. TLS and UAV data integration process on Cloud Compare.

Following the successful completion of the TLS and UAV data integration processes, the meshing process is the next step. The meshing procedure seeks to reconstruct the 3D model created by combining TLS and UAV data. This stage of meshing aims to also bind the data point cloud into a triangular shape and generate a three-dimensional model's surface area. Plugins for Poison Surface Reconstruction are used to generate the mesh. This plugin has a dense point cloud density and works well with closed objects. The parameter used is the octree depth; the greater the value of the octree depth, the finer the mesh results; however, the greater the value used, the greater the time and memory requirements. In this study, a depth of 11 octrees was used to generate a shape that closely resembles the actual situation.

3. Result and Discussion

The build texture is the final step following the formation of the mesh. The objective of this step is to add color and texture to the three-dimensional (3D) model created in the previous step so that it closely resembles the appearance of the real object. The Portion of Visible Sky (qPCV) parameter is used to calculate the illumination from point clouds (or mesh nodes) to provide a texture, color, and light that closely resembles the actual situation on the ground. This parameter works well with objects that have closed shapes; otherwise, the produced light will reach points in the front and back, resulting in unreal (unlikely) results and a lack of contrast. More data will produce smoother results, but it will take longer and require more memory. Figure 4 is a visual representation of the registration, meshing, and texturing processes.

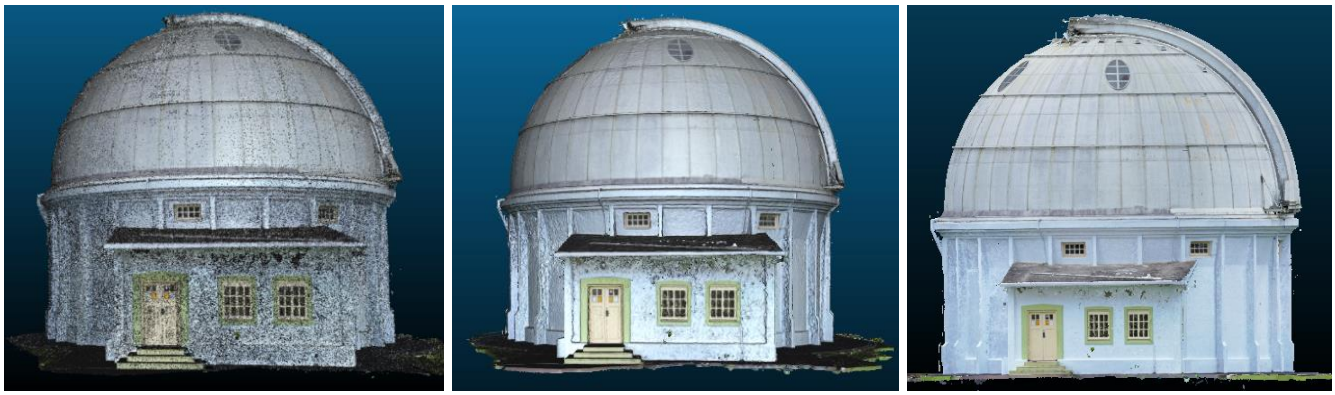

(a) (b) (c)

Source: Analysis, 2022

Figure 4. (a) The results of the TLS and UAV registration processes, (b) meshing using octree depth 11, and (c) texturing objects.

As the final phase of this processing, a solid three-dimensional model of the Bosscha Observatory building is created using the SketchUp Pro after the texture formation stage of TLS and UAV data integration has been completed. As a result of the TLS and UAV data integration process, a point cloud representing a solid 3D model of the building was produced as shown in Figure 5.

The TLS measurement data obtained from Wirnajaya et al. (2019) proved to be insufficient, particularly on the building's roof. This is possible because the acquisition process is influenced by the tool's distance from the object, which impacts the angle at which the object is captured. According to Reshetyuk (2009), if the distance between the instrument and the object is too near, the viewing angle will be reduced. This will have an effect on the roof structure of the Bosscha Observatory, which cannot be modeled accurately. On the other hand, the distance between the tool and the object is an essential planning parameter prior to TLS acquisition. According to Achille et al. (2015), as distance increases, so does resolution. To take measurements of relatively small objects, it is necessary to readjust the correct distance; in this case, the scanned object has a surface area of approximately 552 m2. Even though there are limitations on the measurement distance, the obtained RMSE results are relatively accurate, at 0.015 meters.

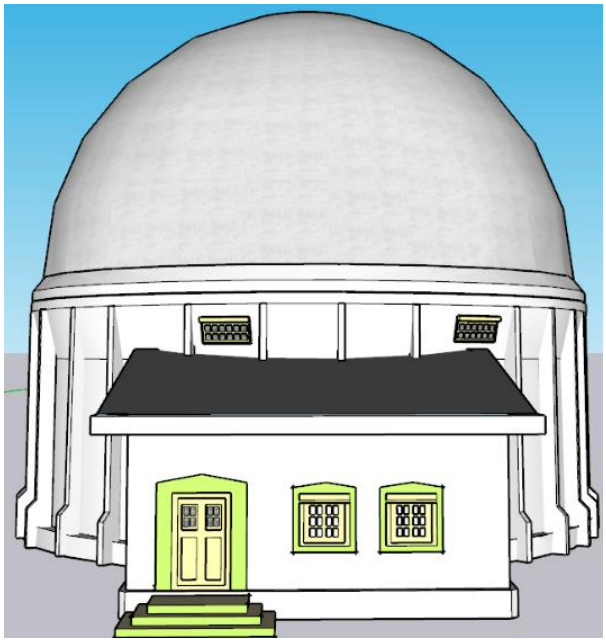

(a)

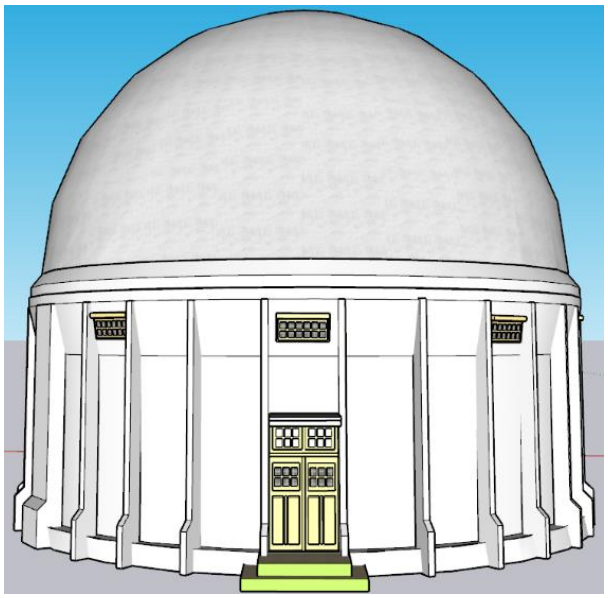

(b)

Source: Analysis, 2022

Figure 5. Bosscha Observatory 3D model (a) front view and (b) rear view created using SketchUp Pro.

Compared to the Maharani et al. (2020), study, the UAV measurement data applied in this research is slightly different. In this study, there were only 334 photos and 31 GCP points, compared to 362 photos and 38 GCP points in Maharani et al. (2020). Due to the lack of overlapping images, the difference in the number of photographs that used will impact the alignment procedure. In Maharani et al. (2020), GCP points were only distributed on the cylindrical portion of the building because the roof was constantly moving for observatories purposes. The variance in GCP points influences the GCP marking procedure. As shown in Figure 6, there is no GCP point available at the building's rear, so this component cannot be properly bonded during the georeferencing procedure. Due to these disparities in data, an RMSE of 0.3 meters was obtained in this study, which is significantly different from the RMSE generated by TLS.

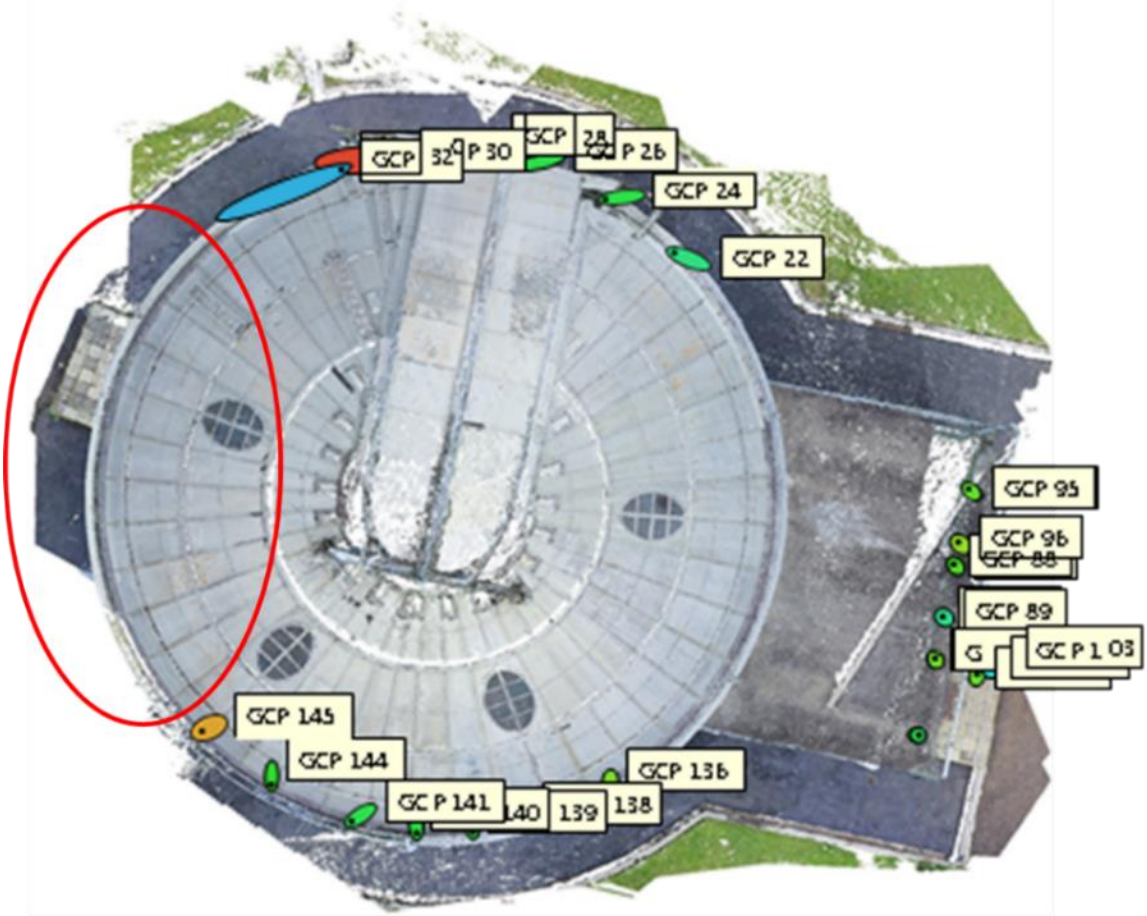

Source: Analysis, 2022

Figure 6. Distribution of GCP points at the Bosscha Observatory. The red circle shows areas that do not have GCP points due to differences in data between this study and Maharani et al. (2020).

In the process of integrating TLS and UAV data, the TLS data is used as a reference because its RMSE value is significantly better than that of the UAV data. However, because the data on the roof of the building cannot accurately represent the actual object, UAV data is utilized to compensate for the shortcomings of the TLS data on the roof. Using the 10 points that are identical in both sets of data, it is possible to integrate the data and obtain an RMSE value of 0.025 meters. Even though the RMSE UAV value is measured in centimeters, the TLS and UAV integration results are measured in millimeters. This is in accordance with the statement Mikrut et al. (2014) that the accuracy of the final object can be improved by combining laser scanning and photogrammetry.

To determine the accuracy of the three-dimensional model derived from the integration of TLS and UAV data, the distance between the integrated model and the TLS registration results on objects visible in both models is compared. Comparing the distance between the two models yields an RMSE of 0.001 meters. The distances between the two models are compared in Table 1.

Based on the differences in distance between the two models, a statistical method was used to assess if the TLS and UAV integration results differed significantly from the TLS data. Calculations for the statistical test were performed using the t-distribution with a 95% confidence interval. The results of statistical test calculations utilizing the t-distribution method indicate that all measurement results from the three-dimensional model of the Bosscha Observatory have been accepted, i.e., they are already within the interval of lower values and upper

values in comparison to the results of the comparison of distance sizes from registration measurements of data processing TLS. This indicates that there is no significant difference between the two data sets.

Table 1. Distances between the two models, where Xi is the size of the average distance of the 3D model as a result of data integration obtained from three measurements; Xi-Yi is the size of the average distance from the registration results of TLS data processing

No	Objects	TLS	Data Integration	Xi-Yi (m)	$(Xi-Yi)^2$ (m)
		Xi (m)	Yi (m)		
1	A01	1.844	1.845	-0.001	0.0000004
2	A02	1.853	1.851	0.002	0.0000028
3	A03	2.371	2.372	0.000	0.0000001
4	A04	2.371	2.370	0.001	0.0000018
5	B01	1.257	1.256	0.002	0.0000028
6	B02	1.257	1.258	-0.001	0.0000010
7	B03	1.594	1.593	0.001	0.0000010
8	B04	1.593	1.592	0.001	0.0000010
9	C01	1.479	1.478	0.000	0.0000001
10	C02	0.938	0.940	-0.002	0.0000054
11	C03	2.095	2.094	0.001	0.0000004
12	C04	1.258	1.259	-0.001	0.0000010
13	C05	1.255	1.253	0.002	0.0000054
14	C06	1.255	1.254	0.001	0.0000018
15	D01	1.598	1.597	0.000	0.0000001
16	D02	1.599	1.598	0.001	0.0000010
17	D03	1.255	1.253	0.001	0.0000018
18	D04	1.256	1.256	0.001	0.0000004
19	E01	1.599	1.598	0.001	0.0000018
20	E02	1.600	1.600	0.000	0.0000000
21	E03	1.685	1.685	0.000	0.0000001
22	E04	1.684	1.683	0.001	0.0000018
23	F01	2.292	2.293	-0.001	0.0000004
24	F02	2.291	2.291	0.000	0.0000000
25	F03	6.016	6.014	0.002	0.0000028
26	F04	0.216	0.214	0.001	0.0000018
27	G01	6.016	6.016	-0.001	0.0000004
28	G02	0.212	0.209	0.003	0.0000071
					1.59524E-06
				RMSE	**0.001263027**

Source: Analysis.2022

4. Conclusion

The results of data integration between TLS and UAV have been implemented successfully and can be used as one of the measurement techniques supporting 3D modeling and compensating for the shortcomings of each tool. The 3D model of the exterior of the Bosscha Observatory produced by the integration process and TLS and UAV data can be used to approximate actual conditions on the ground. This three-dimensional model can be used to create a cylindrical portion of a building and the roof of a hemispherical building; the texture and

color of the building's details, such as windows, doors, and stairs, can be produced with an RMSE error value of 0.025 meters. There is no statistically significant difference between the comparison of the TLS distance size and the TLS and UAV data integration distance size, based on the results of statistical tests. More research is required to determine how to combine different technologies so that the complete shape of an object can be created by utilizing the strengths of each technology.

5. Acknowledgments

This work was supported by Kampus Merdeka Competition Program Research Grant 2021, Geodetic Engineering, Institut Teknologi Nasional Bandung.

6. References

Achille, C., Adami, A., Chiarini, S., Cremonesi, S., Fassi, F., Fregonese, L., & Taffurelli, L. (2015). UAV-Based Photogrammetry and Integrated Technologies for Architectural Applications Methodological Strategies for the After-Quake Survey of Vertical Structures in Mantua (Italy). *Sensors*, *15*(7), 15520–15539. [Crossref]

Ağca, M., Kaya, E., & Yilmaz, H. M. (2020). 3D Modeling of Cultural Heritages with UAV and TLV Systems: A Case Study on The Somuncu Baba Mosque. *ArtGRID - Journal of Architecture Engineering and Fine Arts*, *2*(1), 1–12.

Batur, M., Yilmaz, O., & Ozener, H. (2020). A Case Study of Deformation Measurements of Istanbul Land Walls via Terrestrial Laser Scanning. *IEEE Journal of Selected Topics in Applied Earth Observations and Remote Sensing*, *13*, 6362–6371. [Crossref]

Büyüksalih, G., Kan, T., Özkan, G. E., Meriç, M., Is\in, L., & Kersten, T. P. (2020). Preserving the Knowledge of the Past Through Virtual Visits: From 3D Laser Scanning to Virtual Reality Visualisation at the Istanbul Çatalca İnceğiz Caves. *PFG - Journal of Photogrammetry, Remote Sensing and Geoinformation Science*, *88*(2), 133–146. [Crossref]

Chmutina, K., Jigyasu, R., & Okubo, T. (2020). Editorial for the special issue on securing future of heritage by reducing risks and building resilience. *Disaster Prevention and Management: An International Journal*, *29*(1), 1–9. [Crossref]

Daryono, M. R., Natawidjaja, D. H., Sapiie, B., & Cummins, P. (2019). Earthquake Geology of the Lembang Fault, West Java, Indonesia. *Tectonophysics*, *751*, 180–191. [Crossref]

Dostal, C., & Yamafune, K. (2018). Photogrammetric texture mapping: A method for increasing the Fidelity of 3D models of cultural heritage materials. *Journal of Archaeological Science: Reports*, *18*, 430–436. [Crossref]

Febro, J. D. (2020). 3D Documentation of Cultural Heritage Sites Using Drone and Photogrammetry: a Case Study of Philippine Unesco-Recognized Baroque Churches. *International Transaction Journal of Engineering, Management, & Applied Sciences & Technologies*, *11*(8), 1–14. [Crossref]

Gallay, M., Kaňuk, J., Hochmuth, Z., Meneely, J. D., Hofierka, J., & Sedlák, V. (2015). Large-scale and high-resolution 3-D cave mapping by terrestrial laser scanning: a case study of the Domica Cave, Slovakia. *International Journal of Speleology*, *44*(3), 277–291. [Crossref]

Hu, Q., Wang, S., Fu, C., Ai, M., Yu, D., & Wang, W. (2016). Fine Surveying and 3D Modeling Approach for Wooden Ancient Architecture via Multiple Laser Scanner Integration. *Remote Sensing*, *8*(4), 270. [Crossref]

Klapa, P., Mitka, B., & Zygmunt, M. (2017). Application of Integrated Photogrammetric and Terrestrial Laser Scanning Data to Cultural Heritage Surveying. *IOP Conference Series: Earth and Environmental Science*, *95*(3), 032007. [Crossref]

Kushwaha, S. K. P., Dayal, K. R., Sachchidanand, Raghavendra, S., Pande, H., Tiwari, P. S., Agrawal, S., & Srivastava, S. K. (2020). 3D Digital Documentation of a Cultural Heritage Site Using Terrestrial Laser Scanner - A Case Study. In *Applications of Geomatics in Civil Engineering* (pp. 49–58). Springer Singapore. [Crossref]

Kwoczynska, B., Litwin, U., Piech, I., Obirek, P., & Sledz, J. (2016). The Use of Terrestrial Laser Scanning in Surveying Historic Buildings. *2016 Baltic Geodetic Congress (BGC Geomatics)*, 263–268. [Crossref]

Li, Z., Hou, M., Dong, Y., Wang, J., Ji, Y., & Huo, P. (2021). RESEARCH on the Digital Retention Mechanism of Tibetan Buddhism Architecture Based On UAV and TLS: A Case Study of Baoguang Hall. *{ISPRS} Journal of Photogrammetry and Remote SensingISPRS Annals of the Photogrammetry, Remote Sensing and Spatial Information Sciences*, *VIII-M-1*, 95–100. [Crossref]

Liang, H., Li, W., Lai, S., Zhu, L., Jiang, W., & Zhang, Q. (2018). The integration of terrestrial laser scanning and terrestrial and unmanned aerial vehicle digital photogrammetry for the documentation of Chinese classical gardens A case study

of Huanxiu Shanzhuang, Suzhou, China. *Journal of Cultural Heritage*, *33*, 222–230. [Crossref]

Maharani, M., Charieninna, A., & Nugroho, H. (2020). Identification of photo number effect for 3D modeling in Agisoft software. *IOP Conference Series: Earth and Environmental Science*, *500*(1), 012073. [Crossref]

Manajitprasert, S., Tripathi, N. K., & Arunplod, S. (2019). Three-Dimensional (3D) Modeling of Cultural Heritage Site Using UAV Imagery: A Case Study of the Pagodas in Wat Maha That, Thailand. *Applied Sciences*, *9*(18), 3640. [Crossref]

Mikrut, S., Moskal, A., & Marmol, U. (2014). Integration of Image and Laser Scanning Data Based on Selected Example. *Image Processing & Communications*, *19*(2–3), 37–44. [Crossref]

Murtiyoso, A, Grussenmeyer, P., & Suwardhi, D. (2019). Technical Considerations in Low-Cost Heritage Documentation. *The International Archives of the Photogrammetry, Remote Sensing and Spatial Information Sciences*, *XLII-2/W*, 225–232. [Crossref]

Murtiyoso, Arnadi, & Grussenmeyer, P. (2017). Documentation of heritage buildings using close-range UAV images: dense matching issues, comparison and case studies. *The Photogrammetric Record*, *32*(159), 206–229. [Crossref]

Pan, Y., Dong, Y., Wang, D., Chen, A., & Ye, Z. (2019). Three-Dimensional Reconstruction of Structural Surface Model of Heritage Bridges Using UAV Based Photogrammetric Point Clouds. *Remote Sensing*, *11*(10), 1204. [Crossref]

Reshetyuk, Y. (2009). *Self-calibration and direct georeferencing in terrestrial laser scanning*. KTH.

Themistocleous, K. (2020). The use of UAVs for cultural heritage and archaeology. In *Remote Sensing for Archaeology and Cultural Landscapes* (pp. 241–269). Springer.

Ulvi, A. (2021). Documentation, Three-Dimensional (3D) Modelling and visualization of cultural heritage by using Unmanned Aerial Vehicle (UAV) photogrammetry and terrestrial laser scanners. *International Journal of Remote Sensing*, *42*(6), 1994–2021. [Crossref]

Wirnajaya, Y. R., Kartini, G. A. J., & Nugroho, H. (2019). Pemodelan 3d Kopel Observatorium Bosscha Menggunakan Terrestrial Laser Scanner dengan Metode Cloud To Cloud. *NALARs*, *19*(1), 41. [Crossref]

Wu, C., Yuan, Y., Tang, Y., & Tian, B. (2021). Application of Terrestrial Laser Scanning (TLS) in the Architecture, Engineering and Construction (AEC) Industry. *Sensors*, *22*(1), 265. [Crossref]